Optical spectroscopy of the carrier dynamics in $LaVO_3/SrVO_3$ superlattices

D. W. Jeong,[1] Woo Seok Choi,[1,*] T. D. Kang,[1] C. H. Sohn,[1] A. David,[2] H. Rotella,[2] A. A. Sirenko,[3] Cheol Hyeok Lee,[4] Jae H. Kim,[4] U. Lüders,[2] W. Prellier,[2] Y.-J. Kim,[5] Yun Sang Lee,[6] and T. W. Noh[1,†]

[1] *ReCFI, Department of Physics and Astronomy, Seoul National University, Seoul 151-747, Korea*

[2] *Laboratoire CRISMAT, CNRS UMR 6508, ENSICAEN, 6 Blvd, Maéchal Juin, F-14050 Caen Cedex, France*

[3] *Department of Physics, New Jersey Institute of Technology, Newark, New Jersey 07102, USA*

[4] *Institute of Physics and Applied Physics, Yonsei University, Seoul 120-749, Korea*

[5] *Department of Physics, University of Toronto, Ontario, Canada, M5S 1A7*

[6] *Department of Physics, Soongsil University, Seoul 156-743, Korea*

(Received 8 July 2011; published 22 September 2011)

We investigated the carrier responses of $[(LaVO_3)_{6n}(SrVO_3)_n]$ ($n = 1, 2$, and 4) superlattices using spectroscopic ellipsometry. All the superlattice samples showed an unexpectedly large spectral response in the midinfrared region, which indicated geometrically confined doping near the $LaVO_3$ and $SrVO_3$ interfaces. The intensity of the midinfrared absorption systematically decreased as the superlattice periodicity n increased while the ratio of $LaVO_3$ and $SrVO_3$ layers was kept constant. In addition, we observed that the far-infrared spectral weight of the $n = 1$ superlattice was reduced by up to 30% with decreasing temperature, while the spectral weights of the $n = 2$ and $n = 4$ superlattices were almost temperature independent. This behavior was attributed to the carrier localization effects near the interfaces between $LaVO_3$ and $SrVO_3$.

DOI: 10.1103/PhysRevB.84.115132 PACS number(s): 71.30.+h, 73.21.Cd, 78.20.−e

I. INTRODUCTION

Heterostructures composed of transition metal oxides (TMOs) have been investigated intensively in recent years. Researchers have tried to modify the electronic ground states by stacking ultrathin layers of different TMOs.[1,2] In particular, many efforts have been made to fabricate artificial superlattice (SL) samples by stacking two types of TMO ultrathin layers repetitively. These efforts have sometimes led to the discovery of novel physical phenomena.[3–5] For example, $LaTiO_3/SrTiO_3$ superlattices showed charge leakage from $LaTiO_3$ to $SrTiO_3$ layers, which induced metallic charge carriers around the interface, forming a 2D electron gas.[3,4] In another example, a $LaNiO_3/LaAlO_3$ SL showed a metal-insulator transition (MIT) accompanying antiferromagnetism at low temperatures when the thickness of the $LaNiO_3$ layer decreased below two unit cells.[5]

Among various TMOs, $LaVO_3$ and $SrVO_3$ have been recognized as important building blocks for SLs with intriguing physical properties.[6–8] Bulk $LaVO_3$ is a Mott insulator with V^{3+} ($3d^2$) valence, and the single crystal undergoes a peculiar anisotropic orbital ordering around 141 K, along with antiferromagnetic spin ordering at 143 K.[9,10] Substitution of La with Sr induces filling-controlled MIT, diminishing the anisotropy of the orbital ordering.[9,11] Bulk $SrVO_3$ is a metal with V $3d^1$ configuration that shows strong electronic correlation.[12] When $SrVO_3$ is fabricated in a thin-film form, this material undergoes a band-width controlled MIT as the film thickness decreases below two unit cells, as observed in the recent photoemission study.[13] Combining the peculiar orbital ordering with the dimensional crossover of the physical properties, SLs composed of $LaVO_3$ and $SrVO_3$ are among the most attractive oxide heterostructures to study.

Several intriguing observations have been already reported for $LaVO_3/SrVO_3$ SLs. For example, MIT was observed in $[(LaVO_3)_{6n}(SrVO_3)_n]$ SLs as the SL periodicity n was increased from one to six.[14] Room-temperature ferromagnetism with an insulating interface was also reported for all the series of $[(LaVO_3)_n(SrVO_3)_1]$ SLs as the number of $LaVO_3$ layers n was varied between two and six.[15] A very recent report on the $[(LaVO_3)_6(SrVO_3)_1]$ SL showed a resistivity downturn below 140 K. The authors interpreted this phenomenon as a correlation between the transport properties and a structural phase transition of the $LaVO_3$ film from orthorhombic to monoclinic at the same temperature.[16] Interestingly, a theoretical study of $LaVO_3/SrVO_3$ predicted a double-exchange-driven ferromagnetic insulating ground state along with an orbital density wave gap opening.[17] Until now, however, studies of $LaVO_3/SrVO_3$ SLs have been mostly limited to dc transport and magnetic property measurements. To derive more detailed information on the carrier responses and underlying ground state, optical spectroscopy is highly desirable.

Optical spectroscopy is a useful tool to investigate carrier responses and the electronic structure of oxide heterostructures.[5,18] Most surface sensitive spectroscopy tools use short wavelength light or electrons, whose penetration depths are usually very small (on the order of 1 nm). It is therefore quite difficult to probe the bulk properties or obtain information from the buried interfaces. Optical spectroscopy uses light from the far-infrared to visible region. Since its penetration depth is much longer (on the order of 100 nm to 10 μm), the probing light can penetrate deep into the sample and interact with electrons located near the buried interfaces, providing bulk electrodynamic information. Using spectral weight analysis based on the optical sum rules, optical spectroscopy can provide quantitative information on electrodynamics, such as the number of carriers. In addition, by looking into the spectral features of coherent and incoherent responses in infrared (IR) spectra, we can obtain insights into the electronic band structure near the Fermi energy.[4,19,20]

In this work, we investigated the carrier responses of $LaVO_3/SrVO_3$ SLs using optical spectroscopy. All SL samples showed unusually large spectral weights of midinfrared

(mid-IR) absorption compared to optical spectra derived from an effective medium approximation with simple stacking of $LaVO_3$ and $SrVO_3$. This suggests that there are carrier-doping effects near the $LaVO_3/SrVO_3$ interfaces. The temperature-dependent carrier responses for the $n = 1$ SL showed the characteristics of incoherent transport, whereas the $n = 2$ and $n = 4$ SLs showed weak localization transport behavior. The microscopic disorder at the interface and the strong electron correlations in 3*d* TMOs can be responsible for the incoherent transport properties of $LaVO_3/SrVO_3$ SLs.

II. EXPERIMENTS

We grew $[(LaVO_3)_{6n}/(SrVO_3)_n]$ ($n = 1$, 2, and 4) SLs by depositing the $SrVO_3$ and $LaVO_3$ layers alternatively on a $SrTiO_3$ (001) single-crystal substrate using the pulsed-laser deposition technique. We fixed the ratio between $LaVO_3$ and $SrVO_3$ to investigate the dependence of charge modulation on the SL periodicities.[14] The thicknesses of the SLs were varied from 60 to 80 nm. Details on the preparation can be found in the previous paper by Sheets *et al.*[14] To compare the response of the SLs with that of pure compounds, we also deposited pure $SrVO_3$ and $LaVO_3$ thin films on a $SrTiO_3$ (001) single-crystal substrate using the same growth method.

Structural information of the fabricated SLs was obtained using high-resolution x-ray diffraction (HRXRD, Bruker D8). The optical properties of $LaVO_3/SrVO_3$ SLs were measured using spectroscopic ellipsometry in a broad spectral range. Temperature-dependent far-IR spectra between 12.5–87.5 meV were measured using a homebuilt far-IR spectroscopic ellipsometer attached to a Bruker 66 v/s Fourier transform IR (FT-IR) spectrometer at the U4IR beamline at the National Synchrotron Light Source, Brookhaven National Laboratory. Due to the strong soft phonon mode of the substrate $SrTiO_3$, the spectrum could not be measured below 12.5 meV.[5] The mid-IR (0.07–0.87 eV) and IR to near-UV (0.72–5.6 eV) regions were obtained by GES5E (SOPRA) and VASE (Woollam) ellipsometers, respectively. The angle of incidence of the polarized light was 75° for the far-IR region, and 65, 70, and 75°for the other spectral regions.

We evaluated the complex dielectric function $\tilde{\varepsilon}(\omega)[= \varepsilon_1(\omega) + i\varepsilon_2(\omega)]$ from the spectroscopic ellipsometry data using the following numerical fitting method. Because the SL period was much shorter than the wavelength of the light, the probing light was not sensitive to the detailed structure within the SLs. Therefore we approximated each SL as a single medium with an effective dielectric constant.[4,5,18] The relationship between optical conductivity $\sigma_1(\omega)$ and complex dielectric constant $\tilde{\varepsilon}$ was also used: $\tilde{\varepsilon} = \varepsilon_1 + i\varepsilon_2$, $\sigma_1(\omega) = \omega\varepsilon_2(\omega)/4\pi$. The fact that in-plane $\sigma_1(\omega)$ of the SLs is much larger than the out-of-plane counterparts allows us to probe only the in-plane optical constants of the SLs from the analysis of the ellipsometry data.[4,5] To ensure that the obtained in-plane optical constants were correct, we independently measured the reflectance spectra $R(\omega)$ using a grating spectrophotometer (CARY 5G) with near-normal geometry for the spectral range 0.37–6 eV. We found that the measured $R(\omega)$ agreed with the corresponding value calculated from the ellipsometry data, confirming the validity of our analysis.

III. RESULTS AND DISCUSSION

A. Structural information of the $[LaVO_3)_{6n}/(SrVO_3)_n]$ SLs

Figure 1(a) shows x-ray $\theta - 2\theta$ scan of the $[(LaVO_3)_{6n}/(SrVO_3)_n]$ SLs around the (002) reflection of the $SrTiO_3$ substrate (denoted by $*$). The satellite peaks clearly indicate the doubling of SL periodicity, with increasing SL periodicity from $n = 1$ to $n = 2$ and from $n = 2$ to $n = 4$. The well-defined satellite peaks together with the thickness fringes indicate the good quality of the SLs. However, it should be noted that probable microscopic disorders at the interfaces cannot be recognized easily by x-ray diffraction since this is a volume-averaged probe. Recent transmission electron microscopy (TEM) results on similarly deposited samples showed microscopic atomic steps near the interfaces, although the overall sublattice period seemed to be still satisfactorily defined within the SLs.[21]

Figures 1(b) and 1(c) show schematic diagrams of our $[(LaVO_3)_{6n}/(SrVO_3)_n]$ SLs for $n = 1$ and 2, respectively. Because the SLs were composed of alternate VO_2 and SrO/LaO layers, the number of SrO/LaO layers determined

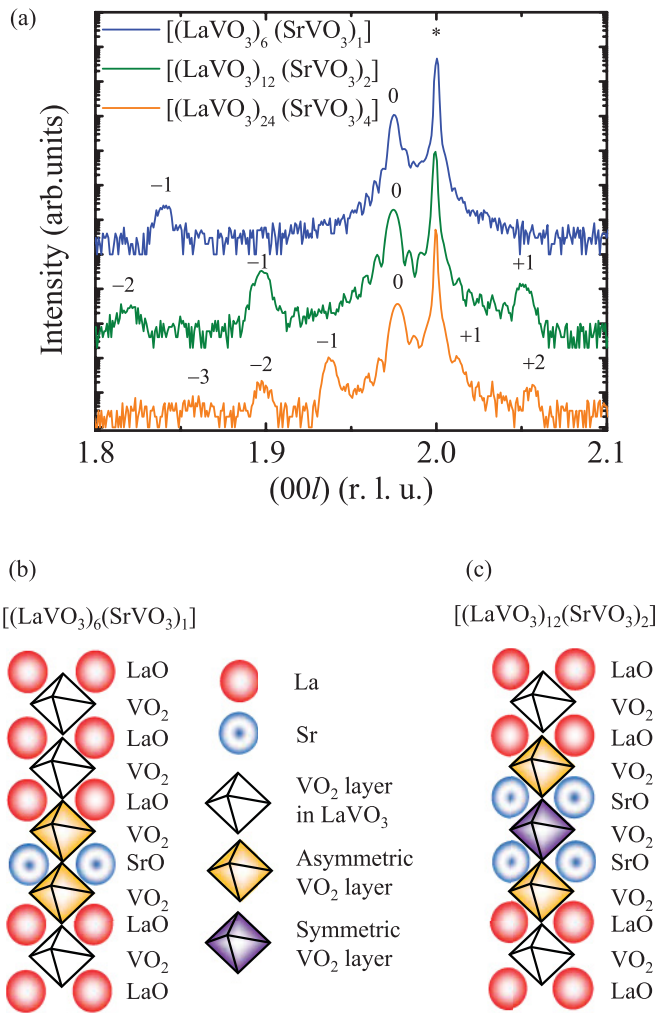

FIG. 1. (Color online) (a) X-ray $\theta - 2\theta$ scan of $[(LaVO_3)_{6n}(SrVO_3)_n]$ ($n = 1$, 2, and 4) superlattices (from top to bottom) around the substrate $SrTiO_3$ with (002) reflection denoted by $*$. Schematic of (b) $n = 1$ and (c) $n = 2$ superlattices.

the unit cell numbers. As displayed in Fig. 1(b), the $n = 1$ SL always contains a VO_2 layer sandwiched by the different layers (SrO and LaO). For convenience, we call this an "asymmetric VO_2 layer".[22] For the $n = 2$ SL, there are two types of VO_2 layers [see Fig. 1(c)]. One is asymmetric, while the other is sandwiched only by SrO layers. This "symmetric VO_2 layer" might have conducting behavior similar to that of the bulk $SrVO_3$. Note that $[(LaVO_3)_6(SrVO_3)_1]$ does not possess any symmetric VO_2 layers. As n increases, the relative ratio of the symmetric VO_2 layers increases.

The V ions in the asymmetric VO_2 layer should have a nominal valence of +3.5. Because the solid-solution $La_{0.5}Sr_{0.5}VO_3$ sample is highly conducting,[9] the asymmetric VO_2 layer should be highly conducting if the real charge state of the V ions is the same as that of V^{+3} ions (see Ref. 5). However, as we will show later, all of our $[(LaVO_3)_{6n}/(SrVO_3)_n]$ SLs are either weakly conducting or insulating. Therefore, we can argue that the charge distribution near the asymmetric VO_2 layer can be extended further into the other VO_2 layers. Some researchers called this "geometrically confined doping."[15,16] However, at present, the conducting behavior due to the charge distribution near the asymmetric VO_2 layer is not known.[6] By investigating the electrodynamics of the $n = 1$ SL compared to the $n = 2$ and $n = 4$ SLs, we can find the intrinsic transport properties due to carriers near the asymmetric VO_2 layer within the SL.

B. Mid-IR absorption of $[LaVO_3)_{6n}/(SrVO_3)_n]$ SLs

To understand the charge carrier responses and electronic structure of the SLs, we looked at the optical spectra below 2.0 eV. Figure 2 shows $\sigma_1(\omega)$ for the $[(LaVO_3)_{6n}/(SrVO_3)_n]$ SLs. The $\sigma_1(\omega)$ of all the SLs have Drude-like features below 0.25 eV and mid-IR absorption around 1.0 eV. The spectra show significant variation in the mid-IR absorption depending on the SL periodicity n, even though the ratio of $LaVO_3$ to $SrVO_3$ is identical for all samples.

To gain more insight, we calculated the effective dielectric constants $\tilde{\varepsilon}_{SL}^{eff}$ of the SLs by using the two-dimensional effective-medium approximation (2D EMA).[19,22] According to the 2D EMA, $\tilde{\varepsilon}_{SL}^{eff}$ can be written as

$$\tilde{\varepsilon}_{SL}^{eff} = \frac{\tilde{\varepsilon}_{LaVO_3} d_{LaVO_3} + \tilde{\varepsilon}_{SrVO_3} d_{SrVO_3}}{d_{LaVO_3} + d_{SrVO_3}},$$

where $\tilde{\varepsilon}_{SL}^{eff}$ and d_A are the complex dielectric constant and thickness of the A layer ($A = LaVO_3$ or $SrVO_3$), respectively. The 2D EMA simulation results are shown with the dashed lines in Figs. 2(a)–2(c). Because our SLs have the same ratio of $LaVO_3$ to $SrVO_3$ layer thicknesses, the 2D EMA simulation predicts that they should all show the same optical responses. However, as shown in Fig. 2(a)–2(c), this simple prediction is not correct.

Although the EMA simulations in Fig. 2 show qualitatively similar features (a Drude response below 0.25 eV and mid-IR absorption), there is a significant difference in the spectral weight between the EMA simulations and our experimental results. To clarify this, we estimated the spectral weight of mid-IR absorption ($SW_{0.25-1.5eV}$) by integrating the optical conductivity spectra in a frequency region between 0.25 and 1.5 eV [$SW_{x\text{-}y} \equiv \int_x^y \sigma_1(\omega)d\omega$]. The result is displayed in the inset of Fig. 2(b). The weights are enhanced by about

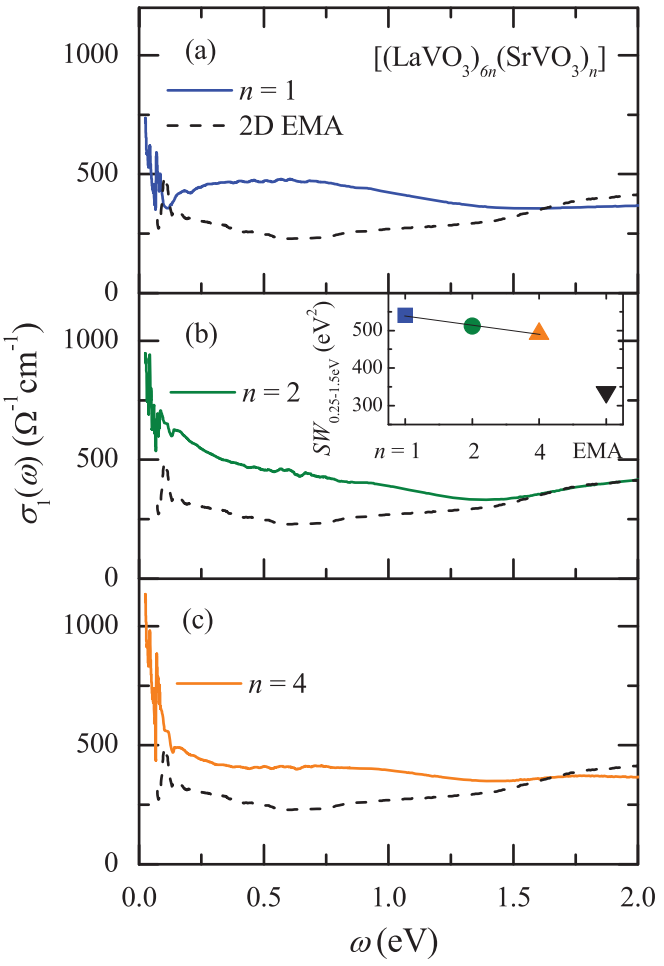

FIG. 2. (Color online) Optical conductivity spectra of $[(LaVO_3)_{6n}(SrVO_3)_n]$ superlattices for (a) $n = 1$, (b) $n = 2$, and (c) $n = 4$ below 2 eV. For comparison, 2D EMA calculation results obtained from the $SrVO_3$ and $LaVO_3$ single layers are also shown by the black dashed line in each superlattice. The inset in (b) shows the spectral weights between 0.25–1.5 eV of our SLs as a function of n. A large enhancement of the spectral weights was observed for all superlattices in the midinfrared region. The enhancements systematically decreased as n increased.

1.4–1.6 times compared to the 2D EMA case, and decreased systematically with increasing SL period.

We suggest that the large enhancement of mid-IR absorption can be associated with the contribution from the interfacial asymmetric VO_2 layers. The 2D EMA is known to be exact when the SL is a stack of two alternating layers with well-defined dielectric constants.[19,22,23] If a $[(LaVO_3)_{6n}/(SrVO_3)_n]$ SL can be viewed as a simple stack of two well-defined layers, its optical constant should follow this 2D EMA result. However, as shown in Fig. 1(b), the VO_2 octahedra in the $n = 1$ SL sample cannot be approximated as a stack of alternating $(VO_2)^0$ and $(VO_2)^{-1}$ layers. In addition, the VO_2 octahedra at the asymmetric layers of all the other SLs cannot be viewed as those of either $LaVO_3$ or $SrVO_3$. The discrepancy between the 2D EMA and experimental results suggests that there were some carrier dynamics changes near the interface.

In the case of $LaTiO_3/SrTiO_3$ SLs, to explain the highly conducting interface, it was argued that electronic

reconstruction should occur at the interface between the $LaTiO_3$ and $SrTiO_3$ layer by spill over of carriers from the Mott-insulating $LaTiO_3$ layer to the band-insulating $SrTiO_3$ layer.[3,24–26] By performing optical spectroscopy on the $LaTiO_3/SrTiO_3$ SLs, Seo *et al.* demonstrated that electronic reconstruction actually occurs at the interface between the $LaTiO_3$ and $SrTiO_3$ layers.[4] Similarly, near the asymmetric VO_2 layer, charge leakage from the $LaVO_3$ side might occur. In fact, a solid solution bulk $La_{1-x}Sr_xVO_3$ sample with $x = 0.168$ shows mid-IR absorption spectra[11,27] that are quite similar to our SL spectra. A previous paper by Sheets *et al.* noted that the length scale of total charge distribution from the dopant charge carriers was longer than the SL periodicity for the $n = 1$ SL.[14] It can be possible that in our $n = 1$ SL, the doped holes in the VO_2 layer spread into most SL regions.[11,14] Based on this geometrically confined doping picture, we can explain the spectral weight change of SLs with increasing n. As the SL periodicity decreases, the relative amount of the asymmetric VO_2 layers increases and the contribution of the doped VO_2 layer to the optical response of SLs should increase.

C. Temperature-dependent far-IR spectra of $[(LaVO_3)_{6n}(SrVO_3)_n]$ SLs

Figures 3(a) and 3(b) show temperature-dependent $\sigma_1(\omega)$ spectra of the $n = 1$ and 4 SLs. In the far-IR region, the room-temperature spectral features are similar for all the SLs. The $LaVO_3$ phonon mode is located near 45 meV. Although all SLs exhibit Drude-like peaks, suggesting free carrier-like background responses, the far-infrared peaks are too broad to represent free carriers. In addition, the temperature dependence of the carrier responses is significantly different. For the $n = 1$ SL, the far-IR spectra systematically decrease with decreasing temperature. For the $n = 2$ and 4 SLs, the temperature dependence is weak. As the temperature decreases, the far-IR spectra of the $n = 2$ and 4 SLs actually increase a little in the low-frequency region. All this spectral behavior indicates that these SLs should be close to the MIT. For a quantitative analysis, we obtained far-IR spectral weight by integrating $\sigma_1(\omega)$ below 86 meV at each temperature, which is normalized by the room-temperature spectral weight, and shown in Fig. 3(c). The spectral weight of the $n = 1$ SL decreases by about 30% with decreasing temperature, while the spectral weight of the $n = 2$ and 4 SLs increases by about 5–10%.

The Anderson localization picture can be adapted to explain the temperature-dependent far-IR spectra of our SLs.[28–30] In an ideal periodic crystal with a barely metallic state, the wave function of the carrier inside the crystal is extended. When we insert atomic-scale disorders into the crystal, the orbital energy near the disorder site can be shifted shrinking the spatial extent of the wave function. In particular, the states originally at the edge of the energy band would have been strongly affected and become localized. As the amount of disorder increases, the metallic sample enters a weakly localized conducting state, followed by an insulating state. Therefore the Anderson localization effect should be significant near the MIT, as for our SLs.

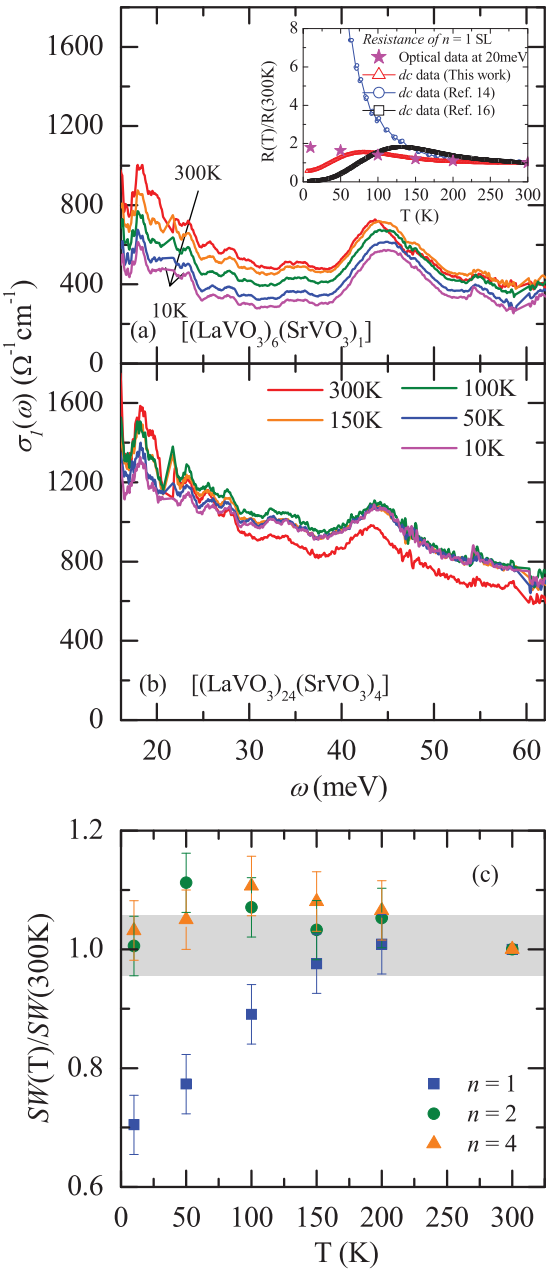

FIG. 3. (Color online) Temperature-dependent far-infrared spectra of (a) $[(LaVO_3)_6(SrVO_3)_1]$ and (b) $[(LaVO_3)_{24}(SrVO_3)_4]$. (c) Temperature-dependent spectral weights normalized to the room-temperature value. While the $[(LaVO_3)_6(SrVO_3)_1]$ superlattice showed a clear decrease of Drude weight with decreasing temperature, the $[(LaVO_3)_{12}(SrVO_3)_2]$ and $[(LaVO_3)_{24}(SrVO_3)_4]$ superlattices showed little change. The inset in (a) shows normalized temperature-dependent resistance data of $[(LaVO_3)_6(SrVO_3)_1]$ superlattice with the data estimated by taking the inverse of optical conductivity value at 20 meV.

Previous TEM studies on $[(LaVO_3)_{6n}/(SrVO_3)_n]$ SLs revealed that there were atomic-scale disorders at the interfaces between $SrVO_3$ and $LaVO_3$, which could play a role as localization centers.[21] Such disorder effects should become stronger as n decreases. As shown in the mid-IR spectra of Fig. 2, more spectral weight of the carriers is located in the mid-IR region than in the far-IR region for all $[(LaVO_3)_{6n}/(SrVO_3)_n]$ SL

samples. Particularly for the $n = 1$ SL, the spectral weight of the mid-IR peak is much stronger than that of the Drude carrier response in the far-IR. Higher density of the atomic scale disorders as observed from the TEM studies and reduced thickness of the $SrVO_3$ layers should be much more effective in localizing the carriers. Therefore, the $n = 1$ SL should behave like an insulating sample, i.e., the far-IR spectra will decrease with decreasing temperature. For the $n = 2$ and 4 SLs, there are more spectral weights in the far-IR region, and the atomic-scale disorder should be less effective in localizing the carriers. The formation of extended wave functions for the whole symmetric VO_2 layers contributes to the charge dynamics, somewhat overcoming the localization effect. Therefore, $n = 2$ and 4 SLs are located in the barely metallic region, so they show slight temperature dependence but metallic responses at low temperatures.

In the inset of the Fig. 3(a), we show the normalized temperature-dependent dc resistance data of $[(LaVO_3)_6(SrVO_3)_1]$ SL with the data estimated by taking the inverse of optical conductivity value at 20 meV. For a comparison, we present the normalized resistance data reported in the Refs. 14 and 16. Note that there is a large variation in the dc transport data and our optical data (shown as the solid stars) is not consistent with any of the dc transport data especially at low temperature. Although some dc data show drastic changes with decreasing temperature, the optical result varies rather smoothly. Usually, dc measurements are strongly influenced by small local percolating conducting channels.[31,32] Particularly for disordered materials, any local percolating conducting channel can short circuit the sample and make it look like a metal.[16,31] In contrast, optical spectroscopy probes the average response of all signals from the sample within the penetration depth.[32] Because the penetration depth of the probing light is much longer than our SL thicknesses, the obtained $\sigma_1(\omega)$ correctly reveals the optical responses of the samples. As reported in earlier works on other materials,[32,33] the dc resistivity values from the optical measurements should be more reliable to those from the dc measurements. Therefore, we claim that our $n = 1$ SL should be in the insulating state near the Anderson localization.

We also compare our results with the ferromagnetic insulating ground state predicted by Jackeli and Khaliullin.[17] At the asymmetric VO_2 interface in the $LaVO_3$ and $SrVO_3$ layers, they theoretically predicted an intriguing ferromagnetic insulating ground state using a quarter-filled t_{2g}-orbital Hubbard model calculation. According to their prediction, the double exchange interaction between V ions with different valences (V^{3+}/V^{4+}) in the asymmetric layer drives this ground state, which is accompanied by a charge or orbital density wave. As the temperature increases, the ferromagnetic correlation should be reduced, exhibiting a more metallic response. Our temperature-dependent far-IR spectra of the $n = 1$ SL are qualitatively consistent with this theoretical prediction. However, we could not observe a clear optical gap induced by orbital and charge density waves, even at the lowest temperature of 10 K. One possibility is that the gap is located below 12.5 meV, which is a spectral region that we could not measure due to strong phonons in the $SrTiO_3$ substrate. The other possibility is the modification of the exchange interaction at the interface due to the disorder, which makes it difficult to observe the suggested confinement effect. Further studies are required for a better understanding of this important issue.

D. Electronic structures of $[LaVO_3)_{6n}/(SrVO_3)_n]$ SLs

Finally, we would like to discuss the interband transitions of $[(LaVO_3)_{6n}/(SrVO_3)_n]$ SLs in the visible and UV region. Figure 4 shows the SL $\sigma_1(\omega)$ for the whole measured spectral region. For comparison, the spectra of $SrVO_3$ and $LaVO_3$ are also displayed. Our measured $\sigma_1(\omega)$ for the $SrVO_3$ and $LaVO_3$ presented here are similar to the previously reported bulk spectra.[12,34,35] All the SLs and pure films show large interband transition peaks above 3 eV. This large peak structure corresponds to the charge transfer transitions between the occupied O $2p$ states and the unoccupied V d states.[35] The charge transfer excitation peaks for $SrVO_3$ and $LaVO_3$ are located at 3.5 and 5.0 eV, respectively, while those for the SLs lie between the two energy scales. There is a systematic variation in the charge transfer transition of the SLs. The charge transfer transition of the $n = 1$ SL is clearly separated into two peaks located at 3.7 and 5.6 eV. Other SLs show multiple but overlapping transitions inside the 3.5–4.5 eV region. Although this evolution is intriguing, we do not understand the origin of this systematic variation at the moment. Further experimental and theoretical investigations of this high-energy feature are desirable.

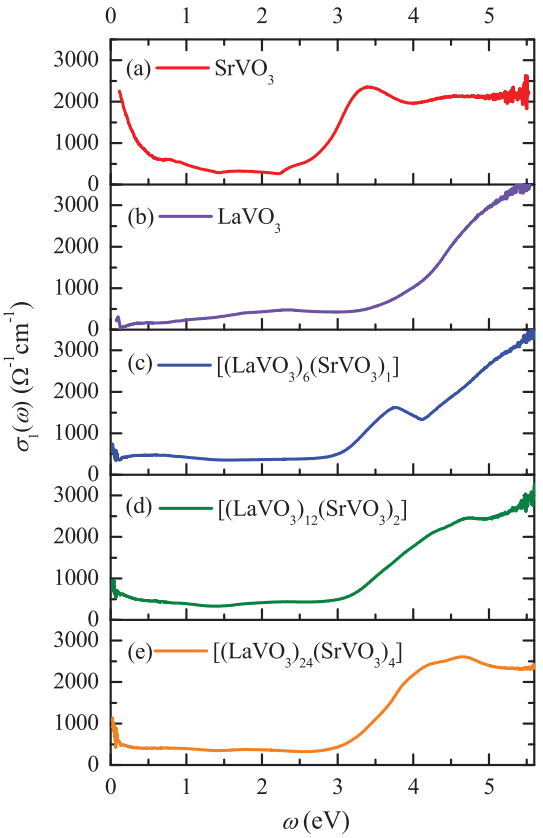

FIG. 4. (Color online) Overall optical conductivity spectra of (a) $SrVO_3$, (b) $LaVO_3$, and $[(LaVO_3)_{6n}(SrVO_3)_n]$ superlattices for (c) $n = 1$, (d) $n = 2$, and (e) $n = 4$.

IV. SUMMARY

We investigated the optical properties of $[(LaVO_3)_{6n}(SrVO_3)_n]$ ($n = 1$, 2, and 4) superlattices. All superlattices showed large mid-infrared absorption due to the geometrically confined carrier doping near the $LaVO_3$ and $SrVO_3$ layers. The spectral weight of the mid-infrared absorption systematically decreased as the superlattice periodicity n increased. The charge density redistribution near the interface layers was suggested as the origin of this phenomenon. Moreover, we observed that the far-infrared spectral weight of the $n = 1$ superlattice decreased with temperature, while the spectral weights of the $n = 2$ and $n = 4$ superlattices were almost temperature independent. This result indicated the formation of an extended state for the $n = 2$ and 4 superlattices within the symmetric VO_2 layers in $SrVO_3$, while the $n = 1$ superlattice showed an incoherent transport.

ACKNOWLEDGMENTS

The authors thank for a valuable discussion with S. S. A. Seo, I. H. Inoue, and Jaehyun Bae. This work was supported by National Research Foundation of Korea (NRF) grants funded by the Korean government (MEST) (Grants Nos. 2009-0080567 and 2010-0020416) and Project STAR (2008-00804). D. W. Jeong was supported by the Korea Student Aid Foundation (KOSAF) grant funded by the Korea government (MEST) (No. S2-2009-000-00046-2). Y.J.K. was supported by the Korean Federation of Science and Technology Societies through the Brainpool program. Use of the National Synchrotron Light Source at the Brookhaven National Laboratory was supported by the US Department of Energy, Office of Science, Office of Basic Energy Sciences, under Contract No. DE-AC02-98CH10886.

*Present address: Materials Science and Technology Division, Oak Ridge National Laboratory, Oak Ridge, Tennessee 37831, USA.
†twnoh@snu.ac.kr

[1] N. Reyren, S. Thiel, A. D. Caviglia, L. F. Kourkoutis, G. Hammerl, C. Richter, C. W. Schneider, T. Kopp, A.-S. Rüetschi, D. Jaccard, M. Gabay, D. A. Muller, J.-M. Triscone, and J. Mannhart, Science **317**, 1196 (2007).
[2] A. Brinkman, M. Huijben, M. van Zalk, J. Huijben, U. Zeitler, J. C. Maan, W. G. van der Wiel, G. Rijnders, D. H. A. Blank, and H. Hilgenkamp, Nat. Mater. **6**, 493 (2007).
[3] A. Ohtomo, D. A. Muller, J. L. Grazul, and H. Y. Hwang, Nature (London) **419**, 378 (2002).
[4] S. S. A. Seo, W. S. Choi, H. N. Lee, L. Yu, K. W. Kim, C. Bernhard, and T. W. Noh, Phys. Rev. Lett. **99**, 266801 (2007).
[5] A. V. Boris, Y. Matiks, E. Benckiser, A. Frano, P. Popovich, V. Hinkov, P. Wochner, M. Castro-Colin, E. Detemple, V. K. Malik, C. Bernhard, T. Prokscha, A. Suter, Z. Salman, E. Morenzoni, G. Cristiani, H.-U. Habermeier, and B. Keimer, Science **332**, 937 (2011).
[6] Y. Hotta, T. Susaki, and H. Y. Hwang, Phys. Rev. Lett. **99**, 236805 (2007).
[7] M. Takizawa, Y. Hotta, T. Susaki, Y. Ishida, H. Wadati, Y. Takata, K. Horiba, M. Matsunami, S. Shin, M. Yabashi, K. Tamasaku, Y. Nishino, T. Ishikawa, A. Fujimori, and H. Y. Hwang, Phys. Rev. Lett. **102**, 236401 (2009).
[8] L. Fitting Kourkoutis, Y. Hotta, T. Susaki, H. Y. Hwang, and D. A. Muller, Phys. Rev. Lett. **97**, 256803 (2006).
[9] S. Miyasaka, T. Okuda, and Y. Tokura, Phys. Rev. Lett. **85**, 5388 (2000).
[10] S. Miyasaka, Y. Okimoto, and Y. Tokura, J. Phys. Soc. Jpn. **71**, 2086 (2002).
[11] J. Fujioka, S. Miyasaka, and Y. Tokura, Phys. Rev. Lett. **97**, 196401 (2006).
[12] H. Makino, I. H. Inoue, M. J. Rozenberg, I. Hase, Y. Aiura, and S. Onari, Phys. Rev. B **58**, 4384 (1998).
[13] K. Yoshimatsu, T. Okabe, H. Kumigashira, S. Okamoto, S. Aizaki, A. Fujimori, and M. Oshima, Phys. Rev. Lett. **104**, 147601 (2010).
[14] W. C. Sheets, B. Mercey, and W. Prellier, Appl. Phys. Lett. **91**, 192102 (2007).
[15] U. Lüders, W. C. Sheets, A. David, W. Prellier, and R. Frésard, Phys. Rev. B **80**, 241102 (2009).
[16] A. David, R. Frésard, P. Boullay, W. Prellier, U. Lüders, and P. E. Janolin, Appl. Phys. Lett. **98**, 212106 (2011).
[17] G. Jackeli and G. Khaliullin, Phys. Rev. Lett. **101**, 216804 (2008).
[18] S. S. A. Seo, M. J. Han, G. W. J. Hassink, W. S. Choi, S. J. Moon, J. S. Kim, T. Susaki, Y. S. Lee, J. Yu, C. Bernhard, H. Y. Hwang, G. Rijnders, D. H. A. Blank, B. Keimer, and T. W. Noh, Phys. Rev. Lett. **104**, 036401 (2010).
[19] W. S. Choi, H. Ohta, S. J. Moon, Y. S. Lee, and T. W. Noh, Phys. Rev. B **82**, 024301 (2010).
[20] A. Dubroka, M. Rössle, K. W. Kim, V. K. Malik, L. Schultz, S. Thiel, C. W. Schneider, J. Mannhart, G. Herranz, O. Copie, M. Bibes, A. Barthélémy, and C. Bernhard, Phys. Rev. Lett. **104**, 156807 (2010).
[21] P. Boullay, A. David, W. C. Sheets, U. Lüders, W. Prellier, H. Tan, J. Verbeeck, G. Van Tendeloo, C. Gatel, G. Vincze, and Z. Radi, Phys. Rev. B **83**, 125403 (2011).
[22] W. S. Choi, D. W. Jeong, S. S. A. Seo, Y. S. Lee, T. H. Kim, S. Y. Jang, H. N. Lee, and K. Myung-Whun, Phys. Rev. B **83**, 195113 (2011).
[23] V. M. Agranovich and V. E. Kravtsov, Solid State Commun. **55**, 85 (1985).
[24] S. S. Kancharla and E. Dagotto, Phys. Rev. B **74**, 195427 (2006).
[25] S. Okamoto and A. J. Millis, Phys. Rev. B **70**, 241104 (2004).
[26] S. Okamoto and A. J. Millis, Nature (London) **428**, 630 (2004).
[27] M. Uchida, K. Oishi, M. Matsuo, W. Koshibae, Y. Onose, M. Mori, J. Fujioka, S. Miyasaka, S. Maekawa, and Y. Tokura, Phys. Rev. B **83**, 165127 (2011).
[28] P. W. Anderson, Phys. Rev. **109**, 1492 (1958).
[29] P. A. Lee and T. V. Ramakrishnan, Rev. Mod. Phys. **57**, 287 (1985).
[30] L. Degiorgi, M. B. Hunt, H. R. Ott, M. Dressel, B. J. Feenstra, G. Grüner, Z. Fisk, and P. Canfield, Europhys. Lett. **28**, 341 (1994).
[31] S. C. Chae, J. S. Lee, S. Kim, S. B. Lee, S. H. Chang, C. Liu, B. Kahng, H. Shin, D.-W. Kim, C. U. Jung, S. Seo, M.-J. Lee, and T. W. Noh, Adv. Mater. **20**, 1154 (2008).
[32] K. H. Kim, J. Y. Gu, H. S. Choi, D. J. Eom, J. H. Jung, and T. W. Noh, Phys. Rev. B **55**, 4023 (1997).
[33] S. S. A. Seo, Z. Marton, W. S. Choi, G. W. J. Hassink, D. H. A. Blank, H. Y. Hwang, T. W. Noh, T. Egami, and H. N. Lee, Appl. Phys. Lett. **95**, 082107 (2009).
[34] T. Arima and Y. Tokura, J. Phys. Soc. Jpn. **64**, 2488 (1995).
[35] R. J. O. Mossanek, M. Abbate, P. T. Fonseca, A. Fujimori, H. Eisaki, S. Uchida, and Y. Tokura, Phys. Rev. B **80**, 195107 (2009).